This full text paper was peer reviewed at the direction of IEEE Communications Society subject matter experts for publication in the IEEE INFOCOM 2007 proceedings.

Optimal Power Control for Multi-hop Software Defined Radio Networks

Yi Shi Y. Thomas Hou

The Bradley Department of Electrical and Computer Engineering, Virginia Tech, Blacksburg, VA

***Abstract*— Software defined radio (SDR) is a revolution in radio technology that promises unprecedented flexibility in radio communications and is viewed as an enabling technology for dynamic spectrum access. This paper investigates how to support user communication sessions by jointly considering power control, scheduling, and flow routing for an SDR-based multi-hop wireless network. We develop a formal mathematical model for scheduling feasibility under the influence of power control. This model extends existing protocol interference model for wireless networks and can be used for a broad class of problems where power control (and thus transmission range and interference range) is part of the optimization space. We formulate a cross-layer optimization problem encompassing power control, scheduling, and flow routing. Subsequently, we develop an efficient solution procedure based on branch-and-bound technique and convex hull relaxation. Using simulation results, we demonstrate the efficacy of the solution procedure and offer insights on the impact of power control on scheduling feasibility, bandwidth efficiency, and bandwidth-footprint product (BFP).**

I. Introduction

Software defined radio (SDR) is a revolution in radio technology that is enabled by recent advances in RF design, signal processing, and communications software [16]. Fundamental characteristics of SDR are that transmitted waveforms are defined by software and that received waveforms are demodulated by software. This is in contrast to traditional hardware-based radios in which processing is done entirely by custom-made hardware circuitry. SDR promises unprecedented flexibility in radio communications and is viewed as an enabling technology for dynamic spectrum access. Its capability has been recognized by the military and commercial sector and is now under intensive research and development by the DoD's Joint Tactical Radio System (JTRS) program and wireless industry.

Since transmitted waveform is defined by software, an SDR is capable of reconfiguring RF (on the fly) and switching to newly-selected frequency bands. From networking perspective, the emergence of SDR offers new challenges in algorithm and protocol design. It is important to realize that an SDR is vastly more powerful and flexible than the so-called *multi-channel multi-radio* (MC-MR) technology that has been actively researched in recent years (see e.g., [1], [6], [10], [11], [15] and reference therein). Note that MC-MR remains *hardware-based* radio technology: each radio can only operate on a single channel at a time and the number of concurrent channels that can be used at a wireless node is limited by the number of radio interfaces. In addition, an MC-MR based wireless network typically assumes there is a set of "common channels" available for all nodes in the network. This assumption is hardly true for SDR networks since each node may have a different set of frequency bands based on its particular location. These important differences between MC-MR and SDR warrant that the algorithm design for an SDR network is substantially more complex than that for MC-MR. From algorithm design perspective, an MC-MR network can be viewed as a special case of an SDR network. Thus, algorithms designed for SDR networks can be easily tailored to address MC-MR networks while the converse is not true.

In this paper, we consider how to jointly perform power control, scheduling, and flow routing for an SDR-based multi-hop wireless network. Specifically, we consider how to support a set of user communication sessions (each with a rate requirement) by jointly optimizing power control, scheduling, and flow routing such that the required radio resource and interference area in the network is minimized. We extend the current "protocol model" for interference modeling (see more discussion in Section II). Since power control directly affects a node's transmission range and interference range, we find that it has profound impact on scheduling feasibility, bandwidth efficiency, and problem complexity. We develop a formal mathematical model for scheduling feasibility under the influence of power control. Based on this model, the joint power control, scheduling, and flow routing problem is subsequently formulated as a *mixed integer nonlinear programming* (MINLP) problem. We develop a solution procedure based on the so-called *branch-and-bound* technique. Using simulation results, we validate this solution procedure and offer additional insights on the impact of power control and variable transmission/interference range on SDR-based wireless networks.

A. Main Contributions

The main contributions of this paper are the following:

- By extending the existing protocol interference model (see Section II for details), we have developed a formal mathematical model for scheduling feasibility under the influence of power control (constraints (C-1'), (C-2'), and (C-3)), which takes into considerations of *variable* transmission and interference ranges. This new model generalizes existing deterministic transmission range and interference range model and can be applied for a broad class of problems where power control is part of the optimization space.
- We have formulated a joint power control, scheduling, and flow routing problem to support a set of user communication sessions in the network with the objective of minimizing radio resource requirement and interference area. Subsequently, we have developed an

0743-166X/07/$25.00 ©2007 IEEE

efficient solution procedure based on branch-and-bound technique and convex hull relaxation to solve this cross-layer optimization problem. The solution obtained via our approach yields a $(1-\varepsilon)$ optimal solution, where ε is a small error tolerance reflecting our desired accuracy in the final solution.

- By applying the solution procedure on sample random networks, we have demonstrated quantitatively that power control has significant impact on scheduling feasibility, bandwidth efficiency, and bandwidth-footprint product (BFP). This confirms the critical need of incorporating power control under the protocol interference model for future wireless network research.

II. Related Work

Related work on MC-MR and its relationship with SDR networks are discussed in Section I. In the rest of this section, we focus our review on cross-layer wireless network research involving interference modeling.

Currently, there are two popular interference models, namely, the *physical model* and the *protocol model.* Under the physical model (e.g., [2], [4], [5], [7], [8], [11]), a transmission is considered successful if and only if the signal to interference and noise ratio (SINR) exceeds a certain threshold, where the interference includes all other concurrent transmissions. Since the calculation of a link's capacity involves not only the transmission power on this link, but also the transmission power on interference links, it is quite difficult to obtain an optimal solution whenever link capacity is involved. In [2], Behzad and Rubin found that for the special case when each node uses the same transmission power, then maximum transmission power should be used. However, for the general case where each node can adjust its transmission power independently, optimal solution is not available. Layered (decoupled) solution approaches were proposed in [4], [5], [7], which yield sub-optimal solutions. In [8], [11], although the lower and upper bounds for transport capacity are obtained (asymptotically), the exact optimal value remains unknown.

Under the so-called protocol model [8], a transmission is considered successful if and only if the receiving node is in the transmission range of the corresponding transmitting node and is out of the interference range of all other transmitting nodes. Under the protocol model, related work can be classified into two categories. In the first category, e.g., [8], [11] (under the so-called "random networks") and [1], [9], [10], [12], [14], [19], the transmission power is fixed. This corresponds to the special case of $Q = 1$ to be discussed later in this paper. Since both the transmission range and interference range are fixed here, the interference relationship among the links are easy to identify. In the second category, i.e., [8], [11] (under the so-called "arbitrary networks") and [3], power control is considered but only for wireless networks with certain special assumptions that may not reflect wireless networks considered in practice. For example, although power control is considered in [3], there is an assumption of no inter-link interference (also called secondary interference [3]) within the network. In [8], [11], power control is considered for the so-called "arbitrary networks," within which the location for each node and its traffic pattern can be arbitrarily changed to optimize transport capacity. Although results for arbitrary networks do yield some theoretical insights, they are far from reflecting what happens for wireless networks in practice, which are mostly random networks [8].

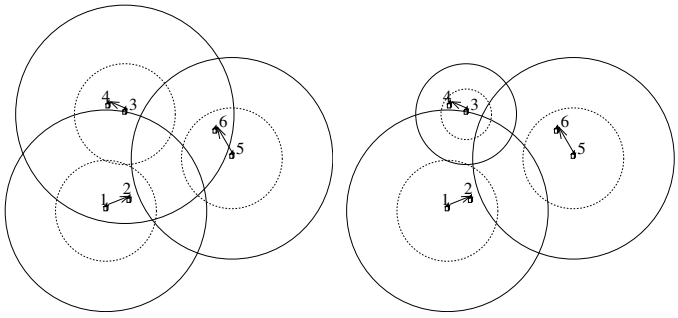

(a) No power control. (b) With power control.

Fig. 1. A 3-link network.

In this paper, we consider the case of power control under the protocol model for general wireless networks (without any special assumptions), i.e., random networks [8]. Such approach captures the most general characteristics of wireless network encountered in practice.

III. Impact of Power Control

In this section, we examine the impact of power control on scheduling feasibility, bandwidth efficiency, and problem complexity in a multi-hop SDR network. But first, we need to have a clear understanding on the notion of transmission and interference ranges in a wireless network as well as the necessary and sufficient condition for successful transmission.

A. Transmission and Interference Ranges

We follow the protocol model as discussed in Section II. In a wireless network, each node is associated with a transmission range and an interference range. Both transmission and interference ranges directly depend on a node's transmission power and propagation gain. For transmission from node i to node j, a widely-used model for propagation gain g_{ij} is

$$g_{ij} = d_{ij}^{-n}\,, \tag{1}$$

where d_{ij} is the physical distance between nodes i and j and n is the path loss index.[1] In this context, we assume a data transmission from node i to node j is successful only if the received power at node j exceeds a power threshold, say α. Suppose node i's transmission power is p and denote the transmission range of this node as $R_T(p)$. Then based on $g_{ij} \cdot p \geq \alpha$ and (1), the transmission range of this node is

$$R_T(p) = \left(\frac{p}{\alpha}\right)^{1/n}\,. \tag{2}$$

Similarly, we assume that an interference power is non-negligible only if it exceeds a threshold, say β at a receiver.

[1] In this paper, we consider a uniform gain model. The case of non-uniform gain model can be extended without much technical difficulty.

Denote the interference range of a node as $R_I(p)$. Then following the same taken as the derivation for the transmission range, the interference range of a node is

$$R_I(p) = \left(\frac{p}{\beta}\right)^{1/n}.$$

Note that the interference range is greater than the transmission range at a node, i.e., $R_I(p) > R_T(p)$ since $\beta < \alpha$. As an example, in Fig. 1(a), we have three unicast communication links $1 \rightarrow 2, 3 \rightarrow 4$, and $5 \rightarrow 6$. For each transmitting node (1, 3, and 5), there are two circles centered around it, with the inner circle (dashed) representing transmission range and the outer circle (solid) representing interference range.

B. Necessary and Sufficient Condition for Successful Transmission

Scheduling for transmission at each node in the network can be done either in time domain or frequency domain. In this paper, we consider scheduling in the frequency domain in the form of frequency bands. In an SDR network, each node has a set of frequency bands that it may use for transmission and receiving. Suppose that band m is available at both node i and node j and denote p_{ij}^m the transmission power from node i to node j in frequency band m. Then to schedule a successful transmission from node i to node j, the following necessary and sufficient condition, expressed as two constraints, must be met. The first constraint (C-1) is that receiving node j must be physically within the transmission range of node i, i.e.,

$$\text{(C-1)} \qquad d_{ij} \leq R_T(p_{ij}^m) = \left(\frac{p_{ij}^m}{\alpha}\right)^{1/n}.$$

The second constraint (C-2) is that the receiving node j must not fall in the interference range of any other node k ($k \in \mathcal{N}$, $k \neq i$) that is transmitting in the same band, i.e.,

$$\text{(C-2)} \qquad d_{jk} \geq R_I(p_{kh}^m) = \left(\frac{p_{kh}^m}{\beta}\right)^{1/n}.$$

where h is the receiving node of node k.

As an example, Fig. 1(a) shows a network with three links ($1 \rightarrow 2, 3 \rightarrow 4$, and $5 \rightarrow 6$). The transmission and interference ranges for each transmitting node (1, 3, and 5) are shown in the figure. Clearly, each receiving node falls in the transmission range of its respective transmitting node. Further, we can see that both receiving nodes 2 and 6 fall in the interference range of node 3. Thus, when link $3 \rightarrow 4$ is using a frequency band m for transmission, link $1 \rightarrow 2$ and link $5 \rightarrow 6$ should not use the same band. It should also be noted that when link $3 \rightarrow 4$ is not using a frequency band m, both link $1 \rightarrow 2$ and link $5 \rightarrow 6$ may use band m. This is because that receiving node 2 does not fall in node 5's interference range and receiving node 6 does not fall in node 1's interference range.

C. Impact of Power Control

In this paper, we investigate the case that each node in an SDR network has power control capability. That is, in addition to being able to transmit at full power P, a node can also transmit at any intermediate power between 0 and P. As one might expect, such freedom on power control has significant impact on design space. In the rest of this section, we illustrate the impact of power control on scheduling feasibility, bandwidth efficiency, and problem complexity.

Scheduling Feasibility. Constraint (C-2) says that a receiving node j (corresponding to transmitting node i on band m) must not fall in the interference range of any other node k that is transmitting in the same band. In the absence of power control, the interference ranges for all the nodes in the network are fixed and there is hardly much we can do once we encounter an infeasibility scenario in scheduling. On the other hand, when power control capability is available, we could adjust the transmission power and thus reduce the interference range of some node so as to achieve scheduling feasibility.

We use an example to illustrate this important point. Recall that in Fig. 1(a), where there is no power control (and thus the transmission ranges and interference ranges for transmitting nodes 1, 3, and 5 are deterministic and shown in the figure), once link $3 \rightarrow 4$ is active (i.e., in transmission) in a frequency band m, then neither link $1 \rightarrow 2$ nor link $5 \rightarrow 6$ shall be active in the same frequency band. If frequency band m is the only band available for these links, then it is impossible to schedule transmissions on links $1 \rightarrow 2$ and $5 \rightarrow 6$. Now consider that each node has the power control capability and can adjust transmission power anywhere in $[0,\ P]$. In this setting, node 3 could reduce its transmission power while still maintaining data transmission to node 4 (see Fig. 1(b)). Now receiving nodes 2 and 6 are no longer in node 3's interference range. As a result of this, both transmitting nodes 1 and 5 can transmit in the same frequency band m simultaneously. In other words, power control could enable scheduling feasibility.

Bandwidth Efficiency. Power control capability has the additional benefit of reducing spectrum bandwidth requirement in the network. This is a direct consequence of the scheduling feasibility benefit discussed above.

Continuing the previous example, in Fig. 1(a), when there is no power control, one frequency band is inadequate to support all three links and we need at least two frequency bands in the network. However, when there is power control, in Fig. 1(b), we only need one frequency band to support all three links. In general, one should expect once power control is employed, the spectrum bandwidth requirement can be reduced significantly for meeting the same communication objective than the case when there is no power control.

Problem Complexity. When power control is allowed, the transmission and interference ranges of a node can be adjusted since both of them are functions of this node's transmission power. It is not hard to realize that the design space for algorithm or optimization solution procedure becomes substantially larger than the case when there is no power control. As a result, mathematical modeling, problem formulation, and solution procedure are also expected to be much more complex and interesting. In the rest of this paper, we explore this problem in the context of multi-hop SDR-based ad hoc networks.

IV. Mathematical Modeling

We consider an ad hoc network consisting of a set of $\mathcal{N}$ nodes. Unlike MC-MR networks where the set of available frequency bands at each node is identical, in an SDR network, the set of available frequency bands at each node depends on its location and may not be the same. For example, at node i, its available frequency bands may consist of bands I, III, and V while at a different node j, its available frequency bands may consist of bands I, IV, and VI, and so forth. More formally, denote $\mathcal{M}_i$ the set of available frequency bands at node i. For simplicity, we assume the bandwidth of each frequency band is W.[2] Denote $\mathcal{M}$ the set of all frequency bands present in the network, i.e., $\mathcal{M} = \bigcup_{i\in\mathcal{N}} \mathcal{M}_i$.

A. Scheduling and Power Control

In Section III, we discussed the necessary and sufficient condition for successful transmission and impact of power control on scheduling feasibility. In this section, we formalize these ideas into a mathematical model in the general context of multi-hop SDR networks.

Suppose that band m is available at both node i and node j, i.e., $m \in \mathcal{M}_{ij}$, where $\mathcal{M}_{ij} = \mathcal{M}_i \bigcap \mathcal{M}_j$. Denote

$$x_{ij}^m = \begin{cases} 1 & \text{If node } i \text{ transmits data to node } j \text{ on band } m, \\ 0 & \text{otherwise.} \end{cases}$$

As mentioned earlier, we consider scheduling in the frequency domain and thus once a band $m \in \mathcal{M}_i$ is used by node i for transmission to node j, this band cannot be used again by node i to transmit to a different node. That is,

$$\text{(C-3)} \qquad \sum_{j\in\mathcal{T}_i^m} x_{ij}^m \le 1 \,, \tag{C-3}$$

where $\mathcal{T}_i^m$ is the set of nodes that are within the transmission range from node i under full power P on band m.

Denote R_T^{max} the maximum transmission range of a node when it transmits at full power P. Then based on (2), we have $R_T^{max} = R_T(P) = \left(\frac{P}{\alpha}\right)^{1/n}$. Thus, we have $\alpha = \frac{P}{(R_T^{max})^n}$. Then for a node transmitting at a power $p \in [0,\ P]$, its transmission range is

$$R_T(p) = \left(\frac{p}{\alpha}\right)^{1/n} = \left[\frac{p(R_T^{max})^n}{P}\right]^{1/n} = \left(\frac{p}{P}\right)^{1/n} R_T^{max} \,. \tag{3}$$

Similarly, denote R_I^{max} the maximum interference range of a node when it transmits at full power P. Then for a node transmitting at a power $p \in [0,\ P]$, its interference range is

$$R_I(p) = \left(\frac{p}{P}\right)^{1/n} R_I^{max} \,. \tag{4}$$

Recall that $\mathcal{T}_i^m$ denotes the set of nodes that are within the transmission range from node i under full power P on band m, we have $\mathcal{T}_i^m = \{j : d_{ij} \le R_T^{max}, j \ne i, m \in \mathcal{M}_j\}$. Similarly, denote $\mathcal{I}_j^m$ the set of nodes that can make interference on node j on band m under full power P, i.e., $\mathcal{I}_j^m = \{k : d_{jk} \le R_I^{max}, \mathcal{T}_k^m \ne \emptyset\}$.

[2]The case of heterogeneous bandwidth for each frequency band can be easily extended.

Note that the definitions of $\mathcal{T}_i^m$ and $\mathcal{I}_j^m$ are both based on full transmission power P. When power level p is below P, the corresponding transmission and interference ranges will be smaller. As a result, it is necessary to keep track of the set of nodes fall in the transmission range and the set of nodes that can produce interference whenever transmission power changes at a node.

Recall the two constraints (C-1) and (C-2) for successful transmission from node i to node j in (3) and (4), respectively, we have

$$d_{ij} \le R_T(p_{ij}^m) = \left(\frac{p_{ij}^m}{P}\right)^{1/n} R_T^{max} \tag{5}$$

$$d_{jk} \ge R_I(p_{kh}^m) = \left(\frac{p_{kh}^m}{P}\right)^{1/n} R_I^{max} \ \ (k \in \mathcal{I}_j^m, k \ne i, h \in \mathcal{T}_k^m). \tag{6}$$

Based on (5) and (6), we have the following requirements for the transmission link $i \to j$ and interfering link $k \to h$:

$$p_{ij}^m \begin{cases} \in \left[\left(\frac{d_{ij}}{R_T^{max}}\right)^n P, P\right] & \text{If } x_{ij}^m = 1, \\ = 0 & \text{If } x_{ij}^m = 0. \end{cases}$$

$$p_{kh}^m \le \begin{cases} \left(\frac{d_{kj}}{R_I^{max}}\right)^n P & \text{If } x_{ij}^m = 1, \\ P & \text{If } x_{ij}^m = 0. \end{cases} \qquad (k \in \mathcal{I}_j^m, k \ne i, h \in \mathcal{T}_k^m) \,.$$

Mathematically, these requirements can be re-written as

$$\text{(C-1')} \ \ p_{ij}^m \in \left[\left(\frac{d_{ij}}{R_T^{max}}\right)^n P x_{ij}^m,\ P x_{ij}^m\right]$$

$$\text{(C-2')} \ \ p_{kh}^m \le P - \left[1 - \left(\frac{d_{kj}}{R_I^{max}}\right)^n\right] P x_{ij}^m \ \ (k \in \mathcal{I}_j^m, k \ne i, h \in \mathcal{T}_k^m) \,.$$

Recall that we consider scheduling in the frequency domain and in (C-3), we state that once a band m is used by node i for transmission to node j, this band cannot be used again by node i to transmit to a different node. In addition, for successful scheduling in frequency domain, the following two constraints must also hold:

- (C-4) For a band $m \in \mathcal{M}_j$ that is available at node j, this band cannot be used for both transmission and receiving. That is, if band m is used at node j for transmission (or receiving), then it cannot be used for receiving (or transmission).
- (C-5) Similar to constraint (C-3) on transmission, node j cannot use the same band $m \in \mathcal{M}_j$ for receiving from two different nodes.

It turns out that the above two constraints are *embedded* in (C-1') and (C-2'). That is, once (C-1') and (C-2') are satisfied, then both constraints (C-4) and (C-5) are also satisfied. This result is formally stated in the following lemma.

Lemma 1: If transmission powers on every transmission link and interference link satisfy (C-1') and (C-2') in the network, then (C-4) and (C-5) are also satisfied.

Proof. Note that (C-4) can be viewed as "self-interference" avoidance constraint where at the same node j, its transmission to another node h on band m interferes its reception from node i in the same band.

- To show that (C-1') and (C-2') lead to (C-4), we first let $k = j$ in (C-2'). Then (C-2') degenerates into $p_{jh}^m \le$

$P - Px_{ij}^m$ since $d_{jj} = 0$. If node j is receiving from node i on band m, i.e., $x_{ij}^m = 1$, then $p_{jh}^m \leq P - Px_{ij}^m = 0$. Since $p_{jh}^m \geq \left(\frac{d_{jh}}{R_T^{max}}\right)^n Px_{jh}^m$ in (C-1'), we have that x_{jh}^m must be 0. That is, if node j is receiving from node i on band m, then node j cannot transmit to a node h in the same band.

- Now suppose node j is transmitting to node h on band m, i.e., $x_{jh}^m = 1$. We will show that this will lead to $x_{ij}^m = 0$. This can be proved by contradiction. That is, if $x_{ij}^m = 1$, then we have just proved in the above paragraph that $x_{jh}^m = 0$. But this contradicts our initial assumption that $x_{jh}^m = 1$. Therefore, x_{ij}^m must be 0. That is, if node j is transmitting to node h on band m, then node j cannot use the same band for receiving from a node i.

Combining the above two results, we have that (C-4) holds.

We now prove that (C-1') and (C-2') also leads to (C-5). Again the proof is based on contradiction. Suppose that (C-5) does not hold. Then node j can receive from two different nodes i and k on the same band m, i.e., $x_{ij}^m = 1$ and $x_{kj}^m = 1$. Note that link $k \rightarrow j$ can be viewed as an interfering link to link $i \rightarrow j$. This corresponds to letting $h = j$ in (C-2'). Then from (C-2'), since $x_{ij}^m = 1$, we have $p_{kj}^m \leq \left(\frac{d_{kj}}{R_I^{max}}\right)^n P$. On the other hand, by (C-1'), we have $p_{kj}^m \geq \left(\frac{d_{kj}}{R_T^{max}}\right)^n P$. However, the above two inequalities cannot hold simultaneously (contradiction) since we have $R_I^{max} > R_T^{max}$. Thus, the initial assumption that (C-5) does not hold is incorrect and the proof is complete. □

The significance of Lemma 1 is that since (C-4) and (C-5) are embedded in (C-1') and (C-2'), *it is sufficient to consider constraints (C-1'), (C-2'), and (C-3) for scheduling and power control.*

B. Flow Routing

We consider an ad hoc network consisting a set of $\mathcal{N}$ nodes. Among these nodes, there is a set of $\mathcal{L}$ active user communication (unicast) sessions. Denote $s(l)$ and $d(l)$ the source and destination nodes of session $l \in \mathcal{L}$ and $r(l)$ the rate requirement (in b/s) of session l. To route these flows from its respective source node to destination node, it is necessary to employ multi-hop due to limited transmission range of a node. Further, to have better load balancing and flexibility, it is desirable to employ multi-path (i.e., allow flow splitting). This is because a single path is overly restrictive and may not yield optimal solution.

Mathematically, this can be modeled as follows. Denote $f_{ij}(l)$ the data rate on link (i, j) that is attributed to session l, where $i \in \mathcal{N}, j \in \mathcal{T}_i = \bigcup_{m \in \mathcal{M}_i} \mathcal{T}_i^m$, and $l \in \mathcal{L}$. If node i is the source node of session l, i.e., $i = s(l)$, then

$$\sum_{j \in \mathcal{T}_i} f_{ij}(l) = r(l) \ . \tag{7}$$

If node i is an intermediate relay node for session l, i.e., $i \neq s(l)$ and $i \neq d(l)$, then

$$\sum_{j \in \mathcal{T}_i}^{j \neq s(l)} f_{ij}(l) = \sum_{k \in \mathcal{T}_i}^{k \neq d(l)} f_{ki}(l) \ . \tag{8}$$

If node i is the destination node of session l, i.e., $i = d(l)$, then

$$\sum_{k \in \mathcal{T}_i} f_{ki}(l) = r(l) \ . \tag{9}$$

It can be easily verified that once (7) and (8) are satisfied, (9) must also be satisfied. As a result, it is sufficient to have (7) and (8) in the formulation.

In addition to the above flow balance equations at each node $i \in \mathcal{N}$ for session $l \in \mathcal{L}$, the aggregated flow rates on each link cannot exceed this link's capacity. Under p_{ij}^m, we have

$$\sum_{l \in \mathcal{L}}^{s(l) \neq j, d(l) \neq i} f_{ij}(l) \leq \sum_{m \in \mathcal{M}_{ij}} c_{ij}^m = \sum_{m \in \mathcal{M}_{ij}} W \log_2 \left(1 + \frac{g_{ij}}{\eta W} p_{ij}^m\right), \tag{10}$$

where η is the ambient Gaussian noise density. Note that the denominator inside the log function contains only ηW. This is due to the use of protocol interference modeling, i.e., when node i is transmitting to node j on band m, then the interference range of all other nodes in this band should not contain node j. Thus, protocol modeling significantly helps to simplify the calculation of link capacity c_{ij}^m.

V. Problem Formulation

Objective Function. In the last section, we presented a mathematical model for constraints on scheduling, power control, and flow routing. Under these constraints, a number of objective functions can be considered for problem formulation. A commonly used objective is to maximize network capacity, which can be expressed as maximizing a scaling factor for all the rate requirements of the communication sessions in the network (see, e.g. [1], [10]). In this paper, we consider another objective called "bandwidth-footprint-product" (BFP), which better characterizes the spectrum and space occupancy for an SDR network. The BFP was first introduced by Liu and Wang in [12]. The so-called "footprint" refers the interference area of a node under a given transmission power, i.e., $\pi \cdot (R_I(p))^2$. Since each node in the network will use a number of bands for transmission and each band will have a certain footprint corresponding to its transmission power, an important objective is to minimize network-wide BFP, which is the sum of BFPs among all the nodes in the network. That is, our objective is to minimize

$$\sum_{i \in \mathcal{N}} \sum_{m \in \mathcal{M}_i} \sum_{j \in \mathcal{T}_i^m} W \cdot \pi (R_I(p_{ij}^m))^2 \ ,$$

which is equal to $\pi (R_I^{max})^2 \sum_{i \in \mathcal{N}} \sum_{m \in \mathcal{M}_i} \sum_{j \in \mathcal{T}_i^m} W \left(\frac{p_{ij}^m}{P}\right)^{2/n}$. Note that although we consider equal bandwidth for each frequency band in the network, the case where each frequency band is of different bandwidth can also be formulated and solved via the solution procedure outlined in the next section.

Discretization of Transmission Powers. For power control, we allow the transmission power to be adjusted between 0 and P. In practice, the transmission power can only be tuned into a finite number of discrete levels between 0 and P. To model this discrete version of power control, we introduce an integer parameter Q that represents the total number of power levels to which a transmitter can be adjusted, i.e., $0, \frac{1}{Q}P, \frac{2}{Q}P, \cdots, P$. Denote $q_{ij}^m \in \{0, 1, 2, \cdots, Q\}$ the integer power level for p_{ij}^m, i.e., $p_{ij}^m = \frac{q_{ij}^m}{Q}P$. Then (C-1'), (C-2'), and (10) can be re-written as follows:

$$q_{ij}^m \in \left[\left(\frac{d_{ij}}{R_T^{max}}\right)^n Qx_{ij}^m,\ Qx_{ij}^m\right] , \quad (11)$$

$$q_{kh}^m \leq Q - \left[1 - \left(\frac{d_{kj}}{R_I^{max}}\right)^n\right] Qx_{ij}^m \quad (k \in \mathcal{I}_j^m, k \neq i, h \in \mathcal{T}_k^m) , \quad (12)$$

$$\sum_{l \in \mathcal{L}}^{s(l) \neq j, d(l) \neq i} f_{ij}(l) \leq \sum_{m \in \mathcal{M}_{ij}} W \log_2 \left(1 + \frac{g_{ij} P}{\eta W Q} q_{ij}^m\right) .$$

Problem Formulation. Putting together the objective function and all the constraints for scheduling, power control, and flow routing, we have formulated an optimization problem in the form of *mixed-integer non-linear programming* (MINLP), which is NP-hard in general. In the next section, we develop a solution procedure based on the branch-and-bound approach [13] and convex hull relaxation.

VI. A Solution Procedure

A. Overview

We find that the so-called *branch-and-bound* approach [13] is most effective in solving our optimization problem. Under this approach, we aim to provide a $(1-\varepsilon)$ optimal solution, where ε is a small positive constant reflecting our desired accuracy in the final solution. Initially, branch-and-bound analyzes partition variables, i.e., all discrete variables and all variables in a non-linear term. For our problem, these variables include all x_{ij}^m's and q_{ij}^m's. Then branch-and-bound determines the value set for each partition variable. That is, we have $x_{ij}^m \in \{0, 1\}$ and $q_{ij}^m \in \{0, 1, 2, \cdots, Q\}$. By using some *relaxation* technique, branch-and-bound obtains a linear relaxation for the original MINLP problem and its solution provides a *lower bound* (LB) to the objective function. As we shall show shortly, this critical step is made possible by the convex hull relaxation for non-linear discrete terms. With the relaxation solution as a starting point, branch-and-bound uses a *local search* algorithm to find a feasible solution to the original problem, which provides an upper bound (UB) for the objective function. If the obtained lower and upper bounds are close to each other, i.e., $LB \geq (1-\varepsilon)UB$, we are done.

If the relaxation errors for non-linear terms are not small, then the upper bound UB could be far away from the lower bound LB. To close this gap, we must have a tighter linear relaxation, i.e., with smaller relaxation errors. This could be achieved by further narrowing down the value sets of partition variables. Specifically, branch-and-bound selects a partition variable with the maximum relaxation error and divides its value set into two sets by its value in the relaxation solution. Then the original problem (denoted as problem 1) is divided into two new problems (denoted as problem 2 and problem 3).

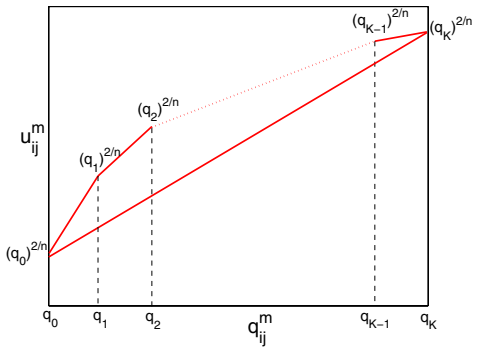

Fig. 2. Illustration of convex hull for a discrete term.

Again, branch-and-bound performs relaxation and local search on these two new problems. Now we have lower bounds LB_2 and LB_3 for problems 2 and 3, respectively. We also have feasible solutions that provide upper bounds UB_2 and UB_3 for problems 2 and 3, respectively. Since the relaxations in problems 2 and 3 are both tighter than that in problem 1, we have $UB_2, UB_3 \leq UB_1$ and $LB_2, LB_3 \geq LB_1$. For a minimization problem, the lower bound of the original problem is updated from $LB = LB_1$ to $LB = \min\{LB_2, LB_3\}$. Also, the best feasible solution to the original problem is the solution with a smaller UB_i. Then the upper bound of the original problem is updated from $UB = UB_1$ to $UB = \min\{UB_2, UB_3\}$. As a result, we now have smaller gap between UB and LB. If $LB \geq (1-\varepsilon)UB$, we are done. Otherwise, we choose a problem with the minimum lower bound and perform partition for this problem.

Note that during the iteration process for branch-and-bound, if we find a problem z with $LB_z \geq (1-\varepsilon)UB$, then we can conclude that this problem cannot provide much improvement on UB. That is, further branch on this problem will not yield much improvement and we can thus remove this problem from further consideration. Eventually, once we find $LB \geq (1-\varepsilon)UB$ or the problem list is empty, branch-and-bound procedure terminates. It has been shown that under very general conditions, a branch-and-bound solution procedure always converges [17]. Moreover, although the worst-case complexity of such a procedure is exponential, the actual running time could be acceptable if all partition variables are integer variables (e.g., the problem considered in this paper).

In the rest of this section, we develop important components in the branch-and-bound solution procedure.

B. Linear Relaxation

During each iteration of the branch-and-bound procedure, we need a relaxation technique to obtain a lower bound of the objective function. For a non-linear discrete term, this can be done by convex hull relaxation. In particular, we replace non-linear discrete term $(q_{ij}^m)^{2/n}$ by a new variable u_{ij}^m and construct its convex hull constraints in the formulation. Suppose $q_{ij}^m \in \{q_0, q_1, \cdots, q_K\}$, where $q_0 = (q_{ij}^m)_L \leq q_1 \leq \cdots \leq q_K = (q_{ij}^m)_U$. The convex hull (see Fig. 2) can be formulated as

$$u_{ij}^m - \frac{(q_K)^{2/n} - (q_0)^{2/n}}{q_K - q_0} q_{ij}^m \geq \frac{q_K (q_0)^{2/n} - (q_K)^{2/n} q_0}{q_K - q_0} ,$$

$$u_{ij}^m - \frac{(q_k)^{2/n}-(q_{k-1})^{2/n}}{q_k-q_{k-1}} q_{ij}^m \le \frac{q_k(q_{k-1})^{2/n}-(q_k)^{2/n}q_{k-1}}{q_k-q_{k-1}} \quad (1 \le k \le K).$$

Similarly, we can replace non-linear discrete term $\log_2\left(1+\frac{g_{ij}P}{\eta WQ}q_{ij}^m\right)$ by a new variable v_{ij}^m and construct its convex hull constraints in the formulation. Thus, we obtain a linear relaxation for the original MINLP formulation.

C. Local Search Algorithm

A linear relaxation for a problem z can be solved in polynomial time. Denote the relaxation solution as $\hat{\psi}_z$, which provides a lower bound to problem z but may not be feasible. We now show how to obtain a feasible solution ψ_z based on $\hat{\psi}_z$.

We use the same routing solution, i.e., let $\mathbf{f} = \hat{\mathbf{f}}$. To obtain a feasible solution, we need to determine the value for $\mathbf{x}$ and $\mathbf{q}$ in solution ψ_z such that the routing solution $\mathbf{f}$ is feasible, i.e., (10) should hold for each link $i \to j$.

Initially, each q_{ij}^m is set as the smallest value $(q_{ij}^m)_L$ in its value set and x_{ij}^m is fixed as 0 or 1 if its value set only have one element 0 or 1, respectively. Based on these q_{ij}^m's, we can compute the capacity $\sum_{m\in\mathcal{M}_i} W\log_2\left(1+\frac{g_{ij}P}{\eta WQ}q_{ij}^m\right)$ for each link $i \to j$. The requirement on a link $i \to j$ is $\sum_{l\in\mathcal{L}}^{s(l)\neq j, d(l)\neq i} f_{ij}(l)$. For each link with a requirement larger than its capacity, we will try to satisfy (10) by increasing q_{ij}^m under its value set limitation. After we do this for all links, then we can calculate the objective value of solution ψ_z. Otherwise, if the requirement of any link cannot be satisfied, then we fail to find a feasible solution and set the objective value as ∞. The details of this local search algorithm is given in [18].

D. Selection of Partition Variables

If the relaxation error for a problem z is not small, the gap between its lower and upper bounds may be large. To obtain a small gap, we generate two new sub-problems z_1 and z_2 from problem z. We hope that these two new problems will have smaller relaxation error, such that the bounds for them can be tighter than bounds for z. Thus, we identify a variable based on its relaxation error.

Since $\mathbf{x}$ variables are more important than $\mathbf{q}$ variables, we first select one of $\mathbf{x}$ variables. In particular, for the relaxation solution $\hat{\psi}_z$, the relaxation error of a discrete variable x_{ij}^m is $\min\{\hat{x}_{ij}^m, 1-\hat{x}_{ij}^m\}$. We choose an x_{ij}^m with the maximum relaxation error among all $\mathbf{x}$ variables and let its value set in problems z_1 and z_2 be $\{0\}$ and $\{1\}$, respectively. It should be note that the new value set of x_{ij}^m may generate limitations on other variables. For example, if the new value set of x_{ij}^m is $\{0\}$, then we have $q_{ij}^m = 0$ based on (11).

If all $\mathbf{x}$ variables are already selected, then we select one of $\mathbf{q}$ variables. In particular, for the relaxation solution $\hat{\psi}_z$, the relaxation error of a discrete variable q_{ij}^m is $\min\{\hat{q}_{ij}^m - \lfloor\hat{q}_{ij}^m\rfloor, \lfloor\hat{q}_{ij}^m\rfloor + 1 - \hat{x}_{ij}^m\}$; the relaxation error of a non-linear discrete term $u_{ij}^m = (q_{ij}^m)^{2/n}$ is $|\hat{u}_{ij}^m - (\hat{q}_{ij}^m)^{2/n}|$; and the relaxation error of a non-linear discrete term $v_{ij}^m = \log_2\left(1+\frac{q_{ij}P}{\eta WQ}q_{ij}^m\right)$ is $\left|\hat{v}_{ij}^m - \log_2\left(1+\frac{q_{ij}P}{\eta WQ}\hat{q}_{ij}^m\right)\right|$. If the maximum relaxation error is related to a discrete variable q_{ij}^m or a non-linear discrete term u_{ij}^m or v_{ij}^m, we choose q_{ij}^m as the branch variable. Assuming the value set of q_{ij}^m in problem z is $\{q_0, q_1, \cdots, q_K\}$, its value set in problems z_1 and z_2 will be $\{q_0, q_1, \cdots, \lfloor\hat{q}_{ij}^m\rfloor\}$ and $\{\lfloor\hat{q}_{ij}^m\rfloor + 1, \lfloor\hat{q}_{ij}^m\rfloor + 2, \cdots, q_K\}$, respectively. Again, the new value set of q_{ij}^m may have limitations on other variables. For example, if the new value set of q_{ij}^m is $\{0\}$, then we have $x_{ij}^m = 0$ based on (11).

TABLE I

EACH NODE'S LOCATION AND AVAILABLE FREQUENCY BANDS FOR THE 20-NODE NETWORK.

Node Index	Location	Available Bands
1	(10.5, 4.3)	I, II, III, IV, V, VI, VII, VIII, IX, X
2	(1.7, 17.3)	II, III, IV, V, VI, VII, X
3	(10.7, 30.8)	I, III, IV, V, VI, VII, VIII, IX, X
4	(10.2, 45.3)	I, III, IV, V, VI, VII, VIII, IX, X
5	(17.8, 4)	I, II, V, VI, VII, VIII, IX
6	(17.2, 15.2)	I, II, IV, VIII
7	(16.9, 30.8)	I, II, III, IV, V, VI, VII, VIII, IX, X
8	(12.3, 47.3)	I, III, IV, V, VII, VIII, IX
9	(28.2, 11.5)	I, III, V, VII
10	(32.1, 13.8)	I, II, III, IV, VI, VII, VIII, IX, X
11	(30.4, 25.6)	I, II, III, V, VI, VIII, IX, X
12	(29.7, 36)	I, II, III, IV, VI, VI
13	(41.7, 3.1)	I, II, III, V, VI, VIII, IX, X
14	(41.7, 3.1)	I, IV, V, VIII, IX, X
15	(43.3, 25.3)	II, III, IV, V, VI, VII, VIII, IX, X
16	(44.1, 42.7)	I, II, IV, VI, VII, VIII, IX, X
17	(49.6, 15.8)	I, II, III, IV, V, VI, VII, VIII
18	(28.7, 2.5)	I, II, III, VI, VII, VIII, IX, X
19	(28, 43.5)	II, IV, V, VI, VIII
20	(5, 46.9)	II, IV, V, VI, VII

TABLE II

SOURCE NODE, DESTINATION NODE, AND RATE REQUIREMENT OF THE 5 SESSIONS.

Source Node	Destination Node	Rate Requirement
7	16	28
8	5	12
15	13	56
2	18	75
9	11	29

VII. SIMULATION RESULTS

In this section, we present some important simulation results. The purpose of this effort is to validate the efficacy of the solution procedure and to offer additional insights on power control that are not obvious from our theoretical development.

For ease of exposition, we normalize all units for distance, bandwidth, rate, and power based on (1) and (10) with appropriate dimensions. We consider a 20-node ad hoc network with each node randomly located in a 50x50 area. An instance of network topology is given in Fig. 3 with each node's location listed in Table I. We assume there are $|\mathcal{M}| = 10$ frequency bands in the network and each band has a bandwidth of $W = 50$. Each node may only have a subset of these frequency bands. In the simulation, this is done by randomly selecting a subset of bands for each node from the pool of 10 bands. Table I shows the available bands for each node.

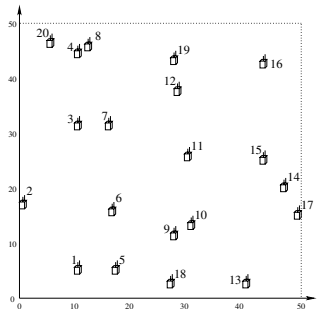

Fig. 3. A 20-node ad hoc network.

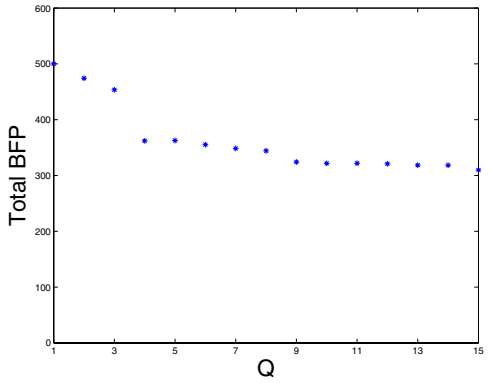

Fig. 4. BFP as a function of discretization levels of power control.

We assume that, under maximum transmission power, the transmission range on each node is 20 and the interference range is twice of the interference range (i.e., 40). Both transmission range and interference range will be smaller when transmission power is less than maximum. The pass loss index n is assumed to be 4. The threshold α is assumed to be $\eta W = 50\eta$. Thus, we have $\beta = \left(\frac{R_T^{max}}{R_I^{max}}\right)^n \alpha W = \frac{50}{16}\eta$ and the maximum transmission power $P = (R_T^{max})^n \alpha W = 8 \cdot 10^6 \eta$.

Within the network, we assume there are $|\mathcal{L}| = 5$ user communication sessions, with source node and destination node randomly selected and the rate of each session is randomly generated within $[10, 100]$. Table II specifies an instance of the source node, destination node, and rate requirement for the 5 sessions in the network.

When the solution procedure in Section VI is applied, the desired approximation error bound ε is set to 0.05, which guarantees that the obtained solution is within 5% from optimum. The running time for each simulation is less than one hour on a Pentium 3.4 GHz machine.[3]

A. Power Control and Level of Granularity on BFP

In this set of simulation results, we apply the solution procedure to the 20-node network described above for different level of power control granularity (Q). Note that $Q = 1$ corresponds to the case of no power control, i.e., a node uses its peak power P for transmission. When Q is sufficiently large, the discrete nature of power control diminishes and power control becomes continuous between $[0,\ P]$.

[3]Note that the solution procedure proposed in this paper is mainly for the purpose of obtaining the theoretical performance bound. In practice, we expect a much simple algorithm with more fast computing time.

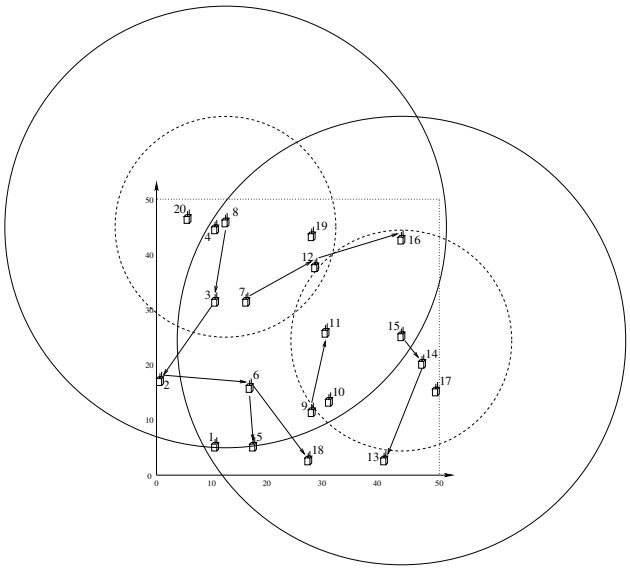

(a) Without power control ($Q = 1$).

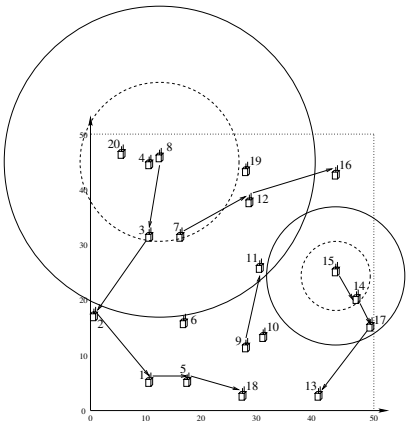

(b) With power control ($Q = 10$).

Fig. 5. Flow routing topology for the 20-node ad hoc network.

Figure 4 shows the results from our solution procedure. First, we note that power control has a significant impact on BFP. Comparing the case when there is no power control ($Q = 1$) and the case of $Q = 15$, we find that there is nearly a 40% reduction in the total BFP. Second, the BFP is a non-increasing function of Q. However, when Q becomes sufficiently large (e.g., 10 in this network setting), further increase in Q will not have much reduction on BFP. This suggests that for practical purpose, the number of required granularity levels to achieve a reasonably good result does not need to be a large number.

To illustrate the difference in routing under different Q, we record the flow routing topology for $Q = 1$ (no power control) and $Q = 10$ in Fig. 5 (a) and (b), respectively. In addition to the obvious difference in flow routing topology starting from

node 2, we also notice that, due to power control, the frequency band used on some link in (a) and (b) are also different. For example, in Fig. 5(a), we plot the transmission range and interference range for nodes 8 and 15. Since there is no power control, node 15 has to use the maximum transmission power P even to nearby node 14. Since node 3 is in the interference range of node 15, nodes 8 and 15 cannot use the same frequency band. On the contrary, in Fig. 5(b), since each node is capable of adjusting transmission power ($Q = 10$), both nodes 8 and node 15 can use smaller transmission powers to achieve the same connectivity and bit rates. As a result, in Fig. 5(b), node 3 is no longer in the interference range of node 15. Thus, in the solution to $Q = 10$, both nodes 8 and 15 are allowed to use the same frequency band. This observation from simulation results validate the benefit on scheduling feasibility brought about by power control.

B. Additional Results on Scheduling Feasibility and Bandwidth Efficiency

To better understand the impact of power control on scheduling feasibility and bandwidth efficiency, we change the available frequency bands in Table I into the following setting. Each node in the 20-node network has an identical set of frequency bands, i.e., $\mathcal{M}_i = \mathcal{M}$. This special case is the setting for MC-MR.

Clearly, when $|\mathcal{M}|$ is very small, feasible solution may not exist for either power control case ($Q = 10$) or no power control case ($Q = 1$). We now increase the available frequency bands $|\mathcal{M}|$ at each node and find that starting from $|\mathcal{M}| = 5$, we can obtain a feasible solution for the power control case ($Q = 10$). However, for $|\mathcal{M}| = 5$, there is still no feasible solution for the no power control case ($Q = 1$).

It is not hard to see that if we continue to add available frequency bands into the network, we will eventually have a feasible solution for the no power control case ($Q = 1$). In our simulation results, we find that only when $|\mathcal{M}| = 9$, we find a first feasible solution for the no power control case. Recall that we only need $|\mathcal{M}| = 5$ for a feasible solution with power control. This example verifies that not only power control offers greater design space for scheduling feasibility, it also conserves the number of frequency bands for the network to be operational.

VIII. Conclusions

In this paper, we investigated how to support user communication sessions by jointly performing power control, scheduling, and flow routing for an SDR-based multi-hop wireless network. We developed a formal mathematical model for scheduling feasibility under the influence of power control. This model extends the existing so-called protocol model for wireless networks where transmission range and interference range are deterministic and thus can be used for a broad class of problems where power control (and thus transmission range and interference range) is part of the optimization space. We formulated a cross-layer optimization problem encompassing power control, scheduling, and flow routing and developed an efficient solution procedure based on branch-and-bound technique and convex hull relaxation. Through simulation results, we demonstrated quantitatively that power control and variable transmission/interference range have significant impact on scheduling feasibility, bandwidth efficiency, and bandwidth-footprint product. This validates the critical need of incorporating power control under the existing protocol interference modeling for future wireless network research.

Acknowledgements

This work has been supported in part by NSF Grant CNS-0627436.

References

[1] M. Alicherry, R. Bhatia, and L. Li, "Joint channel assignment and routing for throughput optimization in multi-radio wireless mesh networks," in *Proc. ACM Mobicom,* pp. 58–72, Cologne, Germany, Aug. 28–Sep. 2, 2005.

[2] A. Behzad and I. Rubin, "Impact of power control on the performance of ad hoc wireless networks," in *Proc. IEEE Infocom,* pp. 102–113, Miami, FL, March 13–17, 2005.

[3] R. Bhatia and M. Kodialam, "On power efficient communication over multi-hop wireless networks: joint routing, scheduling and power control," in *Proc. IEEE Infocom,* pp. 1457–1466, Hong Kong, China, March 7–11, 2004.

[4] C.C. Chen and D.S. Lee, "A joint design of distributed QoS scheduling and power control for wireless networks," in *Proc. IEEE Infocom,* Barcelona, Catalunya, Spain, April 23–29, 2006.

[5] R.L. Cruz and A.V. Santhanam, "Optimal routing, link scheduling and power control in multi-hop wireless networks," in *Proc. IEEE Infocom,* pp. 702–711, San Francisco, CA, March 30–April 3, 2003.

[6] R. Draves, J. Padhye, and B. Zill, "Routing in multi-radio, multi-hop wireless mesh networks," in *Proc. ACM Mobicom,* pp. 114–128, Philadelphia, PA, Sep. 26–Oct. 1, 2004.

[7] T. Elbatt and A. Ephremides, "Joint scheduling and power control for wireless ad-hoc networks," in *Proc. IEEE Infocom,* pp. 976–984, New York, NY, June 23–27, 2002.

[8] P. Gupta and P.R. Kumar, "The capacity of wireless networks," *IEEE Transactions on Information Theory,* vol. 46, no. 2, pp. 388–404, March 2000.

[9] K. Jain, J. Padhye, V. Padmanabhan, and L. Qiu, "Impact of interference on multi-hop wireless network performance," in *Proc. ACM Mobicom,* pp. 66–80, San Diego, CA, Sep. 14–19, 2003.

[10] M. Kodialam and T. Nandagopal, "Characterizing the capacity region in multi-radio multi-channel wireless mesh networks," in *Proc. ACM Mobicom,* pp. 73–87, Cologne, Germany, Aug. 28–Sep. 2, 2005.

[11] P. Kyasanur and N.H. Vaidya, "Capacity of multi-channel wireless networks: impact of number of channels and interfaces," in *Proc. ACM Mobicom,* pp. 43–57, Cologne, Germany, Aug. 28–Sep. 2, 2005.

[12] X. Liu and W. Wang, "On the characteristics of spectrum-agile communication networks," in *Proc. IEEE DySpan,* pp. 214–223, Baltimore, MD, Nov. 8–11, 2005.

[13] G.L. Nemhauser and L.A. Wolsey, *Integer and Combinatorial Optimization,* John Wiley & Sons, New York, NY, 1999.

[14] K. Ramachandran, E. Belding-Royer, K. Almeroth, and M. Buddhikot, "Interference-Aware Channel Assignment in Multi-Radio Wireless Mesh Networks," in *Proc. IEEE Infocom,* Barcelona, Catalunya, Spain, April 23–29, 2006.

[15] A. Raniwala and T. Chiueh, "Architecture and algorithms for an IEEE 802.11-based multi-channel wireless mesh network," in *Proc. IEEE Infocom,* pp. 2223–2234, Miami, FL, March 13–17, 2005.

[16] J.H. Reed, *Software Radio: A Modern Approach to Radio Engineering,* Prentice Hall, May 2002.

[17] H.D. Sherali and W.P. Adams, *A Reformulation-Linearization Technique for Solving Discrete and Continuous Nonconvex Problems,* Kluwer Academic Publishers, Dordrecht/Boston/London, Chapter 8, 1999.

[18] Y. Shi and Y.T. Hou, "Optimal power control for multi-hop software defined radio networks," Technical Report, the Bradley Department of Electrical and Computer Engineering, Virginia Tech, Blacksburg, VA, July 2006. Available at http://www.ece.vt.edu/thou/Research.html.

[19] J. Tang, G. Xue, C. Chandler, and W. Zhang, "Interference-aware routing in multihop wireless networks using directional antennas," in *Proc. IEEE Infocom,* pp. 751–760, Miami, FL, March 13–17, 2005.